NASA Technical Memorandum 101415

Fracture Toughness Computational Simulation of General Delaminations in Fiber Composites

T.E. Wilt
Akron University
Akron, Ohio

P.L.N. Murthy
Cleveland State University
Cleveland, Ohio

and

C.C. Chamis
Lewis Research Center
Cleveland, Ohio

Presented at the
29th Structural Dynamics and Materials Conference
cosponsored by the AIAA, ASME, AHS, and ASC
Williamsburg, Virginia, April 18-20, 1988

NASA

FRACTURE TOUGHNESS COMPUTATIONAL SIMULATION OF GENERAL DELAMINATIONS IN FIBER COMPOSITES

T.E. Wilt
Akron University
Akron, Ohio 44325

P.L.N. Murthy
Cleveland State University
Cleveland, Ohio 44115

and

C.C. Chamis
National Aeronautics and Space Administration
Lewis Research Center
Cleveland, Ohio 44135

SUMMARY

A procedure is described to computationally simulate composite laminate fracture toughness in terms of strain energy release rate (SERR). It is also used to evaluate the degradation in laminate structural integrity in terms of displacements, loss in stiffness, loss in vibration frequencies and loss in buckling resistance. Specific laminates are selected for detailed studies in order to demonstrate the generality of the procedure. These laminates had center (midplane) delaminations, off-center delaminations, and pocket delaminations (center and off-center) at the free-edge and center delaminations at the interior. The laminates had two different thicknesses and were made from three different materials. The results obtained illustrate the effects of delamination on the laminate structural integrity and on the laminate strain energy release rate (composite fracture toughness).

INTRODUCTION

Free-edge regions and discontinuities in composite laminates are often sites at which steep interlaminar stress gradients are present. These steep stress gradients are intrinsic to the anisotropic heterogeneous structure of the laminate (plies are oriented in different directions) and develop when the laminate is subjected to mechanical and/or environmental loads. Interlaminar stresses are important considerations in laminate design because they contribute to fatigue degradation of the laminate by causing delamination extensions. In a previous study (refs. 1 to 3), a unique computational procedure was developed to simulate fracture toughness for delamination in composite laminates. Recently this computational procedure has been extended to simulate fracture toughness for general delaminations and/or transply cracks in composite laminates. The objective of the present paper is to describe the extended method and its application to select delamination cases of practical significance.

The extended procedure consists of judicious use of: (1) finite element modeling, (2) multipoint constraints, and (3) composite mechanics. The delaminations are represented by double nodes which are connected with appropriate multipoint constraints. The sublaminates (groups of undelaminated plies) on either side of these discontinuities are modeled with plate finite elements. The stiffnesses of the elements are generated using composite mechanics. These stiffnesses, (membrane, coupled, and bending) are generated directly from constituent material properties where environmental effects can be included. The delamination extensions are initiated by progressively releasing the appropriate multipoint constraints defined at a later section.

The procedure is subsequently used to computationally simulate fracture toughness in terms of strain energy release rate (SERR). It is also used to evaluate the degradation in laminate structural integrity in terms of variations in displacements, loss in stiffness, loss in vibration frequencies and loss in buckling resistance. Specific laminates were selected for detailed studies in order to demonstrate the generality of the procedure. These laminates had center (midplane) delaminations, off-center delaminations, and pocket delaminations (center and off-center). The laminates had two different thicknesses and were made from three different materials. The details are described in reference 4. In this paper we briefly describe the computational simulation procedure, present typical results and discuss the significance of these results to composite laminates and composite structures.

COMPUTATIONAL SIMULATION PROCEDURE

Laminates Investigated

The laminates investigated had an aspect ratio of length to width of 4 to 1, with the thickness varying according to the number of plies in the laminate, figure 1. In the first model, the laminate is divided into two equal sublaminates in order to simulate the center delamination. This model is used for the $[\pm 30/90]_S$ 6-ply center and the $[\pm 30/90/\pm 30/90_2]_S$ 14-ply center delamination cases.

In the second 14-ply model the laminate is subdivided into five sublaminates. By including these additional sublaminates, a laminate with multiple delaminations through the thickness can be modeled. This model is used for the $[\pm 30/90/\pm 30/90_2]_S$ 14-ply offset case.

The second model is quite general because by varying the thicknesses of the two sublaminates and the corresponding number of plies in each, the delamination can be placed at any location through the thickness of the laminate. For example, instead of having the delamination located at the center of the laminate, it could be placed at some distance offset from the center. The delamination nomenclature to be used in this paper is defined in figure 2.

Finite Element Models

Several finite element models were constructed in order to simulate delamination between plies in the laminate. The sublaminates on either side of the delamination plane were modeled using 4-noded isoparametric quadrilateral plate elements, QUAD4 in MSC/NASTRAN with nodes located at the

midplane of the sublaminate as shown in figure 3. The QUAD4 elements are used in conjunction with PSHELL cards that define the thickness of the sublaminate and the associated material properties of the QUAD4 elements. The PSHELL card allows the input of material properties such as the membrane, bending, and coupling relationships that correspond to the properties of the group of plies that the sublaminate is representing.

The values for the material properties were computed by using the Integrated Composite Analyzer (ICAN) program (ref. 5). This is a computer program which utilizes composite micromechanics, along with laminate theory, to calculate the associated composite properties for a given sublaminate configuration. ICAN also allows for different temperature and moisture conditions to be used, thus allowing these effects to be included in the analysis if desired. ICAN is run with the desired group of plies in the sublaminate to provide input values for the finite element membrane, bending and coupling stiffnesses.

Boundary Conditions

The boundary conditions on the models are chosen so that realistic end testing conditions. In the cases of strain energy release rate, buckling load, and axial stiffness, one end of the specimen is clamped with all 6° of freedom restrained while the other end is only restrained to prevent any out-of-plane (z direction) translation. In the frequency analysis, one end remains clamped and the other end is pinned with both x and z translations restrained.

Multipoint Constraints

Since the laminate has been divided into sublaminates, it is necessary to tie these sublaminates together. This is accomplished by connecting the nodes of adjacent sublaminates through the use of multipoint constraint equations (fig. 4). These equations are implemented into the finite element model through a series of MPC (multipoint constraint) cards located in the bulk data deck. The constraint equations used form a linear relationship between a series of nodes allowing the laminate to extend and bend according to plate theory. When all of the constraint equations are in effect for each and every node, all of the sublaminates combine and act as one intact laminate with no delaminations present. By releasing the constraints between the nodes, the nodes are free to move independent of one another. It is through the use of multipoint constraints and bending-extensional coupling of the plate elements that progressive delamination is simulated in the composite laminates.

The equation for multipoint constraints are as follows: one node is chosen to contain the independent degrees of freedom and all remaining nodes degrees of freedom are considered dependent on the first node. The equations are written so as to allow bending in both the x and y directions, enabling plate behavior to be modeled. A group of five equations are written for each node; three translations and two rotations. The third rotation, that in the z-direction, is fixed for the entire model to eliminate any stiffness singularities of the QUAD4 plate elements used here.

Thus, referring to figure 4, the following constraint equations are formed. The first group of equations for the x and y translations enforce the constraints displacements are linearly continuous between plies, i.e.,

no slippage of the plies. The through-the-thickness translations between each ply are assumed to be equal, i.e., no separation of plies, and the rotations through the thickness are constant.

Types of Delamination

The types of delaminations considered are described below:

Uniform free edge delamination. - In the free-edge delamination studies, two patterns of release sequences are used. The first is shown in figure 5. This particular pattern will be referred to as uniform delamination. As can be seen in figure 5, the delamination begins in the center of each edge of the composite laminate. The nodes are then relased (refs. 1), according to the prescribed pattern indicated by the numbers, in a sequential manner proceeding from the center, down along the edge, and then inward towards the center of the laminate. As shown in the figure, the delamination grows slowly along the edge in the form of an element by element propagation. Then the delamination begins to propagate inward, it does so in a uniform manner whereby entire rows of elements are released simultaneously. This type of delamination is similar to that observed in experiments (ref. 6). The free-edge delamination observed assumes a slightly parabolic shape as the delamination initially grows inward. But, as the delamination proceeds further inward, the parabola flattens out and propagates as a uniform shape. Thus, the basis for the type of propagation used here.

Pocket free-edge delamination. - Small pockets of delamination are usually observed along the free-edge. These pockets would develop after the formation of transply cracks. These transply cracks are also a matrix dominated failure mode, as is interply delamination, and occur in those plies whose strength in the load direction is also matrix dominated. The crack forms completely through the thickness of the ply and usually terminates at the interface with the adjacent ply. At this point, the crack spreads along the ply interface in the form of interply delamination. Thus, the transply cracks result in the initial formation of small pockets of delamination at the crack location. Since small pockets seem to be the type in which interply delamination initiates, it is desirable to also simulate this type to see if it would lead to any significant changes in the predicted delamination effects. This is referred to as the pocket delamination type, figure 6. This type of delamination is somewhat idealized, in that the pockets initially are introduced at the center of each free-edge and then uniformly grow along the edge. The remaining elements are then released between the pockets to simulate the individual pockets coalescing into one continuous delamination along the free-edge. From this point on, the delamination propagates inward as before.

Interior delamination. - One additional delamination type is used to investigate the effects of a delamination that occurs in the interior of the composite laminate. The motivation for including this type of delamination is that it could be induced by an impact of some object on the surface of the laminate. As shown in figure 7, the delamination is initially taken as a small square region in the center of the laminate. This delamination is then propagated along the length and then outward towards the free-edges of the laminate.

Strain Energy Release Rate

The use of strain energy release rate (SERR) is one of the commonly used indicators of how susceptible a particular laminate is to delamination. In effect, the strain energy release rate gives a measure of the amount of energy that is required to propagate a defect in the laminate. This amount of energy has been used to evaluate the delamination fracture toughness of the laminate. As the area of interply delamination is progressively increased, the greater the amount of energy released, the more likely the particular damage state will occur for that laminate configuration. The strain energy release rate allows a direct comparison of the damage tolerance between different laminate materials, configurations and geometries. It provides the capability to see particular delamination influences, such as, location effects, material property dependence, etc.

The methods used to calculate the strain energy release rate are many. One of those commonly used is the crack closure method. In this method, nodal displacements and nodal forces, at the crack tip location, are used to determine the amount of work required to close the crack which has been extended by an incremental amount. This in turn provides a measure of the amount of energy available to propagate the crack further.

This approach is a local level approach since the amount of energy expended by the local displacements and forces at the crack front are used to calculate the corresponding strain energy release rate. The objective of this study is to characterize the effects of delamination using the overall structural response of the laminate, a global approach is used to calculate the strain energy release rate.

In the global approach, the work expended is calculated by considering the nodal displacements and nodal forces located at the loaded end of the laminate. The nodal forces are the applied loads used in the tensile loading case, and the nodal displacements are those predicted by the finite element analysis at the same end nodes at which the load is applied. The equation given below is that used to calculate the strain energy release rate G,

$$G = \frac{dW}{dA} = \frac{1}{2} \frac{(Fu_2) - (Fu_1)}{\Delta A}$$

W Exteral work (force times and displacement)

F Loads applied at end nodes

U_1 Displacements at end nodes before ΔA

U_2 Displacements at end nodes after ΔA

ΔA Change in delaminated area

which simply stated, is the incremental change in work divided by the incremental change in the delaminated area. The applied tensile load F remains constant and the delaminated area is the amount of additional surface area that is "opened" for that node release sequence. The nodes are released according to the types of delaminations discussed previously.

RESULTS AND DISCUSSION

Cases Evaluated

The various cases evaluated are summarized in Table 1. The evaluation includes variation in material properties, laminate configurations and laminate thicknesses. Three different materials systems are used to study fiber and matrix influences. These systems are AS-graphite fiber with intermediate modulus high strength epoxy (AS/IMHS) and with high modulus high strength epoxy (AS/HMHS), and S-glass fibers with intermediate modulus high strength epoxy (S-G/IMHS). In the first two systems, intermediate and high modulus matrix materials are used with a graphite fiber to see the influence of matrix stiffness variation. The last system, S-G/IMHS, has a lower stiffness fiber giving a much lower laminate overall stiffness as compared to the graphite fiber systems. Both fiber and matrix properties for these composites are listed in Table 2.

Uniform Free-Edge Delamination

Computer plots of free-edge center and pocket delaminations are shown in figure 8. Laminate cross sections for free-edge center and offset delaminations are shown in figure 9. These computer plots illustrate, in part, the effectiveness of the computational simulation for representing various types of free-edge delamination.

Results for SERR (G) versus percent areas delaminated for the six ply laminate with center delamination are shown in figure 10 for the AS/IMHS, AS/HMHS and S-G/IMHS composites. The significant points to be observed in figure 10 are: (1) free-edge delamination under tensile load is not catastrophic since no rapid increase in G occurs with progressively larger delaminated area, (2) substantial free-edge delamination under tensile load- ing will probably occur once delamination initiated since the curves for G are relatively flat versus percent area delaminated greater than 10 percent, (3) the SERR is significantly influenced by the matrix modulus in the composite, the higher the matrix modulus the greater the resistance to free-edge delamination assuming equal strength, and (4) the fiber modulus significantly influences the SERR, the higher the fiber modulus the more prone is the composite laminate to free-edge delamination AS/IMHS versus S-G/IMHS. It is interesting to note that these effects are substantial and should be easy to discriminate experimentally.

Corresponding results are shown in figure 11 for the 14-ply laminate with center delaminations and in figure 12 for the 14-ply laminate with offset delaminations. The results in these two figures show the same trends as those in figure 10. Comparing the results in figures 11 and 12, it can be seen that the SERR (G) is the same for center and for offset multiple delaminations. The conclusion to be drawn is that multiple free-edge delaminations can occur simultaneously in certain laminates under tensile loading.

Free-Edge Pocket Delaminations

The results for SERR for the 6-ply laminate with free-edge center pocket delaminations are shown in figure 13. The sequence in which the nodes were released to simulate this type of delamination is shown in figure 6. The

results in figure 13 show that free-edge pocket delaminations is unstable and will rapidly coalesce (rapid increase in G at ΔA = 20 percent) into continuous delamination along the edge. Comparing these curves with those in figure 11, the SERR is the same for inward delamination propagation for both cases. The 14-ply laminate center and offset free-edge pocket delaminations exhibit similar behavior.

It was previously mentioned that free-edge pocket delaminations are likely to initiate from transply cracks. It may be concluded from the results in figure 12 then, that free-edge delaminations initiate as pocket delaminations which coalesce into continuous delaminations and which propagate inward as continuous delaminations.

Interior Delamination

The results for SERR for the 6-ply laminate with interior delamination under tensile loading are shown in figure 14. The sequence in which the nodes are released in order to simulate this type of delamination is shown in figure 7. The results in figure 14 demonstrate that interior delamination in a tensile stress field is benign since the SERR (G) is negligible until the interior delamination has extended to the free edges. This is so because the interply layer has negligible contribution to the laminate axial stiffness. Two points are worth noting: (1) no degradation in structural integrity in tensile stress fields does not necessarily imply absence of interior delaminations. This is consistent with experimental observations (ref. 7) and (2) the effects of interior delaminations on composite laminate structural integrity must also be evaluated in the presence of shear, compression and bending stress fields for actual structural applications. The methods described herein are applicable for these stress fields as well.

Effects of Delamination on Laminate Structural Integrity

The effects of delamination on laminate structural integrity (structural integrity degradation) were evaluated by plotting changes in the structural integrity variables such as: (1) increases in displacement, (2) loss in stiffness, (3) loss in vibration frequency, and (4) loss in buckling load versus percent of delaminated area. Plots for all of these were generated for both laminates (6- and 14-ply) for each of the delamination types (center and offset), and for each of the three composite systems (AS/IMHS, AS/HMHS and S-G/IMHS). These plots are numerous and are not included here. One typical plot is shown in figure 15 for buckling load. This plot is similar to those for axial stiffness and vibration frequency and complementary to that for end displacement. Collectively, the results indicate the following general trends: (1) practically linear decrease in the structural integrity variables with increasing percent in delaminated area, (2) the rate of structural integrity degradation (dx) with respect to delaminated area (dA), (dx/dA) is less than 20 percent, (3) the higher the fiber modulus in the composite the higher the degradation rate, (4) the higher the matrix modulus in the composite the lower the degradation rate, and (5) the vibration frequency exhibits the lowest degradation rate while the axial stiffness is the greatest. One important conclusion from the above discussion is that the computational simulation procedure described herein is effective in evaluating the structural integrity degradation of laminates with various types of delaminations. Furthermore, since the method is <u>not</u> restricted to the cases studied it should also be equally as effective for composite structures in general.

CONCLUDING REMARKS

The salient results of an investigation of the fracture toughness of general delaminations in fiber composites are as follows:

1. A procedure has been developed to computationally simulate the fracture toughness (strain energy release rate (SERR)) in fiber composites with various delaminations).

2. Free-edge delaminations do not lead to laminate catastrophic fracture under tensile loadings.

3. Multiple free-edge delaminations are possible in thick laminates. The SERR for single and multiple delaminations is about the same.

4. Pocket free-edge delaminations are unstable. They rapidly coalesce into continuous delaminations along the free-edge.

5. Interior delaminations have no effect on laminate fracture toughness in tensile stress fields until they extend to the free edges. Then, their effects are the same as those of free-edge delaminations.

6. Laminate structural integrity in terms of: axial stiffness, buckling load and vibration frequency, degrades linearly with increasing delamination area. The rate of degradation is less than 20 percent. It is the highest for axial stiffness and the lowest for vibration frequency.

7. Increasing the fiber modulus increase the degradation rate of the laminates structural integrity while increasing the matrix modulus has the opposite effect.

REFERENCES

1. Murthy, P.L.N.., and Chamis, C.C.: Interlaminar Fracture Toughness: Three-Dimensional Finite Element MOdeling for End-Notch and Mixed-Mode Flexure. (NASA TM_87138), 1985.

2. Murthy, P.L.N.; and Chamis, C.C.: Composite Interlaminar Fracture Toughness 3-D Finite Element Modeling for Mixed Mode I, II, and III Fracture," (NASA TM-88872), 1986.

3. Murthy, P.L.N. and Chamis, C.C.: Fracture Toughness Computational Simulation of Edge Delaminations in Fiber Composites. Presentation at the AIAA/ASME/ASCE/AHS 28th SDM Conference, April 6-8, 1987, Monterey, California.

4. Wilt, T.E.: Computational Simulation of Composite Structures With and Without Damage. Master's Thesis, The University of Akron, Akron, Ohio, May 1988.

5. Murthy, P.L.N. and Chamis, C.C.: Integrated Composite Analyzer (ICAN): Users and Programmers Manual. NASA TP 2515, 1986.

6. Sun, C.T., et. al.: Report NADC-85068-60, Purdue University, West Lafayette, Indiana, 1985.

7. Porter, T.R.: Environmental Effects on Defect Growth in Composite Materials. NASA CR 165213, 1981.

Table 1. - Summary of Cases Studied

Cases	Static load tensile u E/E_0 G	Buckling load, P_{cr}/P_0	Vibration frequency ω/ω_0
Free-edge delamination			
6-Ply center [+30/90]s			
AS/IMHS	* * *	*	*
AS/HMHS	* * *	*	*
S-G/IMHS	* * *	*	*
14-Ply center [+30/90/+30/90_2]s			
AS/IMHS	* * *	*	*
AS/HMHS	* * *	*	*
S-G/IMHS	* * *	*	*
14-Ply offset [+30/90/+30/90_2]s			
AS/IMHS	* * *	*	*
AS/HMHS	* * *	*	*
S-G/IMHS	* * *	*	*
Interior delamination			
6-Ply center [+30-/90]s			
AS/IMHS	*		
AS/HMHS	*		
S-G/IMHS	*		

TABLE 2. - FIBER AND MATRIX PROPERTIES

(a) Fiber

Property	AS	S-G
Density, ρ_m, lb/in.^{3}	0.063	0.090
Longitudinal modulus, E_{f11}, 10^6 psi	31.0	12.4
Transverse modulus, E_{f22}, 10^6 psi	2.0	12.4
Longitudinal shear modulus, [a]G_{f12}, 10^6 psi	2.0	5.17
Transverse shear modulus, [a]G_{f23}, 10^6 psi	1.0	5.17
Longitudinal Poisson's ratio, ν_{f12}	0.20	0.20
Transverse Poisson's ratio, ν_{f23}	0.25	0.20

(b) Matrix

Property	IMHS	HMHS
Density, ρ_m, lb/in.^{3}	0.044	0.045
Elastic modulus, E_m, 10^6 psi	0.50	0.75
Shear modulus, G_m,[a] 10^6 psi	-----	-----
Poisson's ratio, ν_m	0.35	0.35

[a]Shear property is an estimate only, $G_m = Em/[2(1+\nu_m)]$.

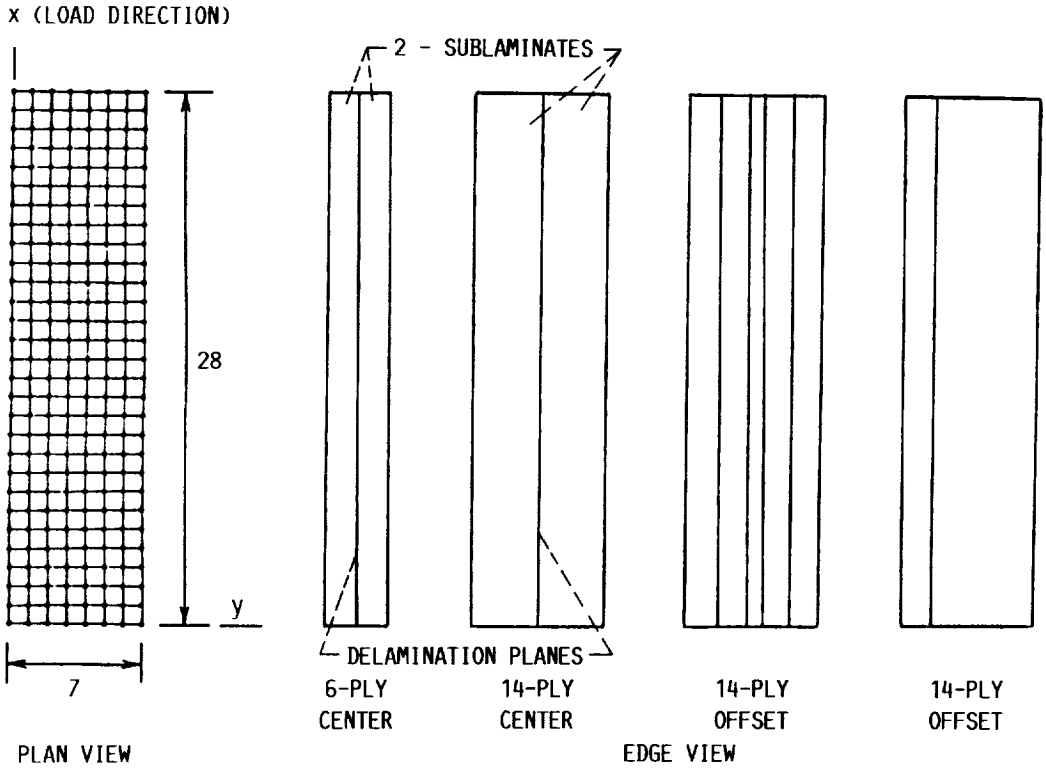

FIGURE 1. - LAMINATES MODELED PLAN (FINITE ELEMENT MESH) AND EDGE VIEWS (DIMENSIONS IN INCHES).

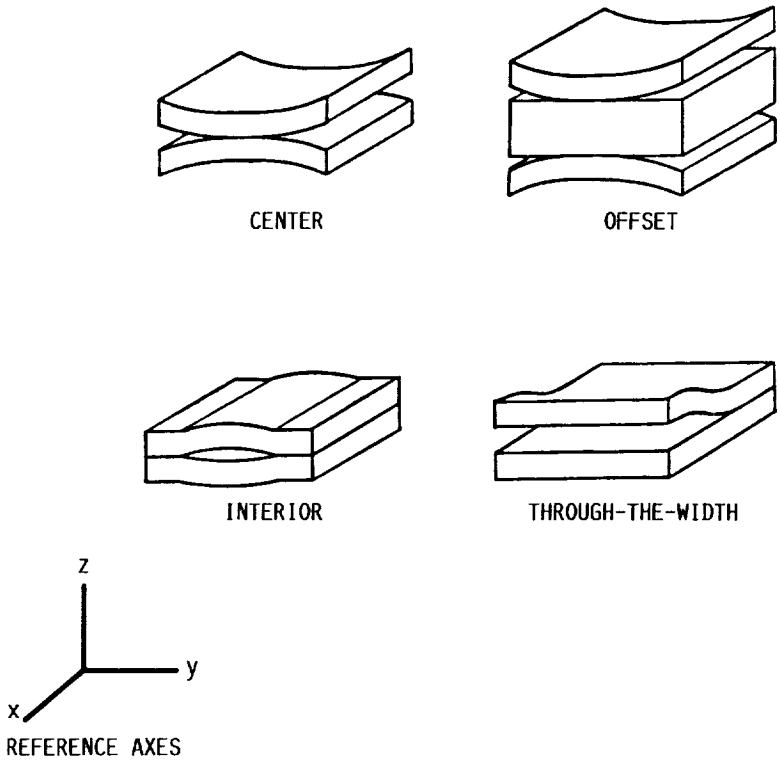

FIGURE 2. - DELAMINATION NOMENCLATURE.

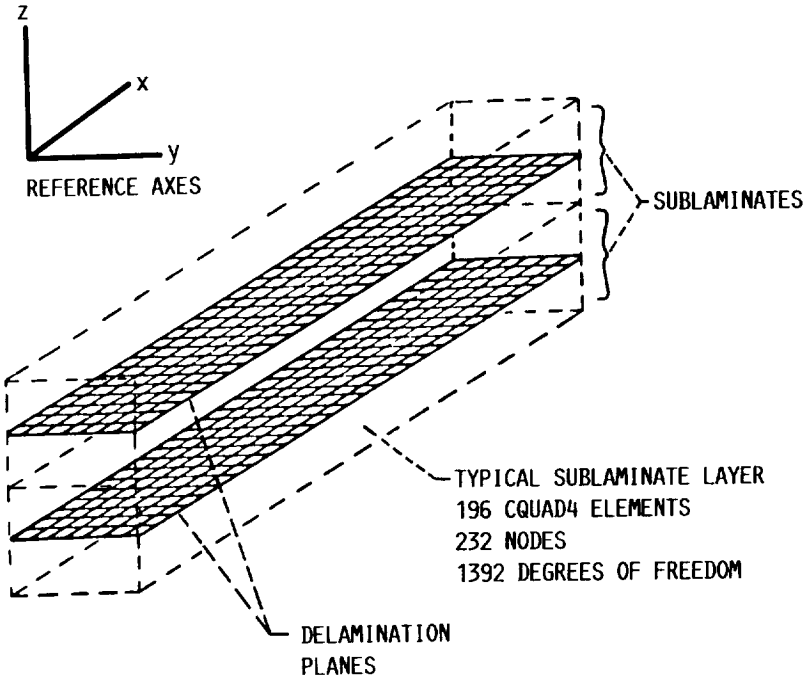

FIGURE 3. - LAMINATE FINITE ELEMENT MODEL.

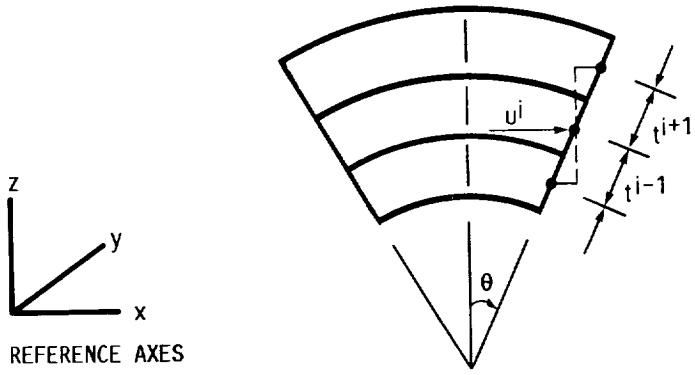

IN-PLANE DISPLACEMENTS

$$u^{i+1} = u^i + \theta_y t^{i+1} \qquad u^{i-1} = u^i - \theta_y t^{i-1}$$

$$v^{i+1} = v^i + \theta_x t^{i+1} \qquad v^{i-1} = v^i - \theta_x t^{i-1}$$

TRANSVERSE DISPLACEMENTS

$$w^{i+1} = w^i = w^{i-1}$$

ROTATIONS

$$\theta^{i+1} = \theta^i = \theta^{i-1}$$

FIGURE 4. - MULTI-POINT CONSTRAINTS.

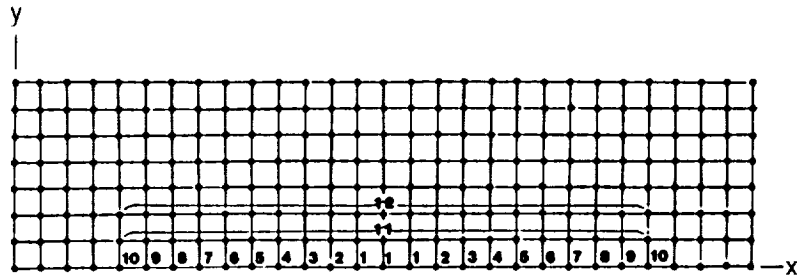

FIGURE 5. - UNIFORM DELAMINATION NODE RELEASE SEQUENCE NUMBERED.

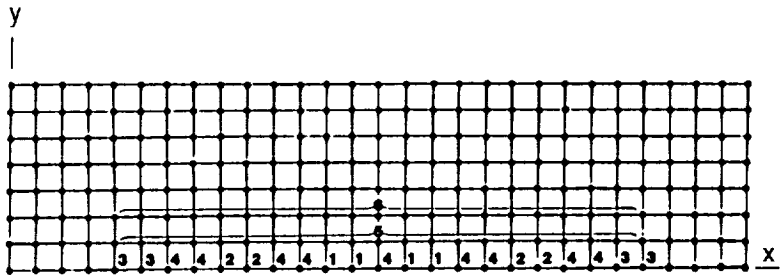

FIGURE 6. - POCKET DELAMINATION NODE RELEASE SEQUENCE NUMBERED.

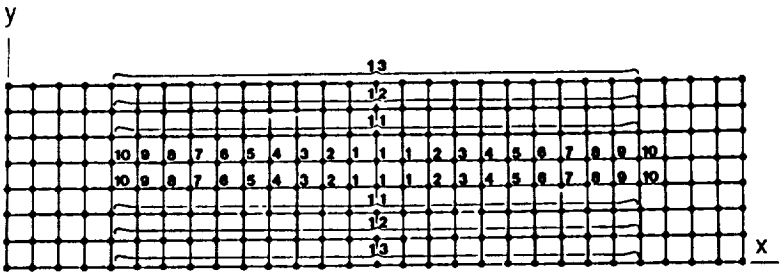

FIGURE 7. - INTERIOR DELAMINATION NODE RELEASE SEQUENCE NUMBERED.

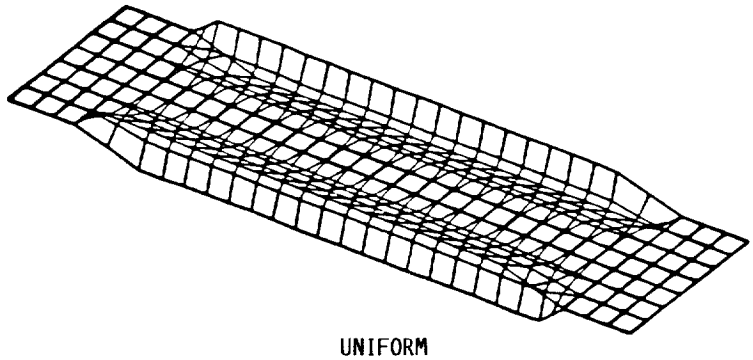

UNIFORM

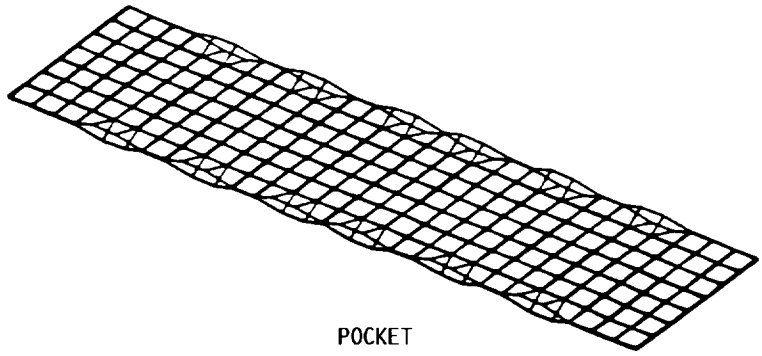

POCKET

FIGURE 8. - MID-PLANE DELAMINATION SIMULATION RESULTS.

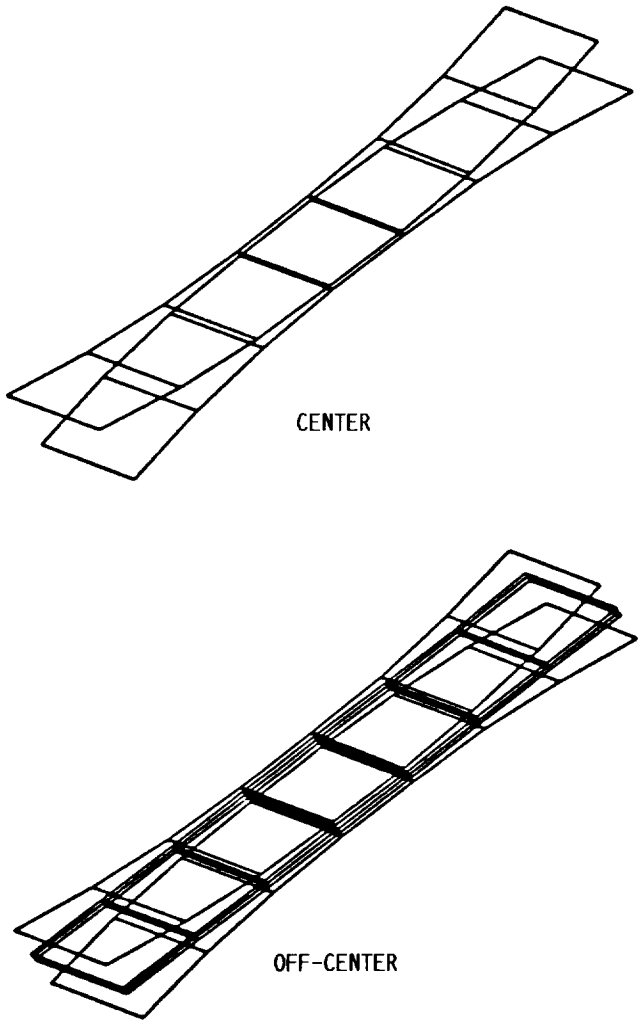

FIGURE 9. - DELAMINATED LAMINATE CROSS-SECTIONS.

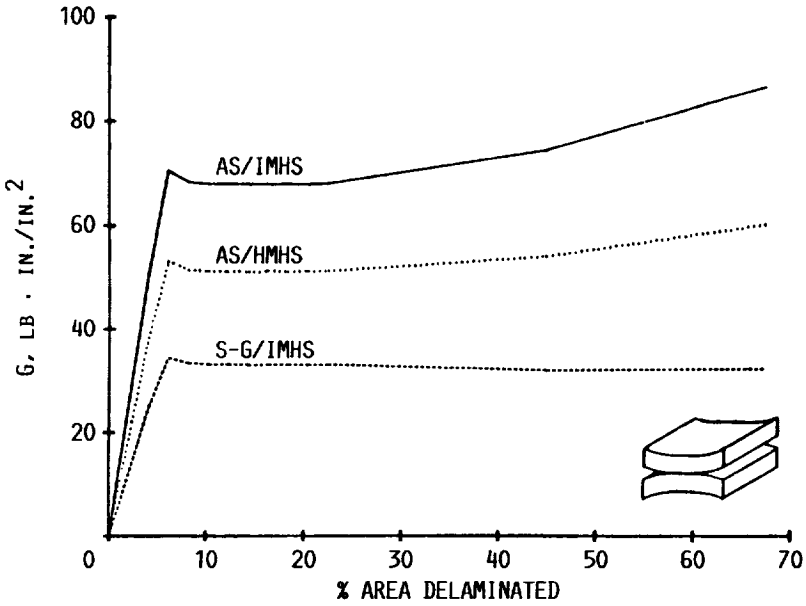

FIGURE 10. - STRAIN ENERGY RELEASE RATE 6-PLY CENTER DELAMINATION.

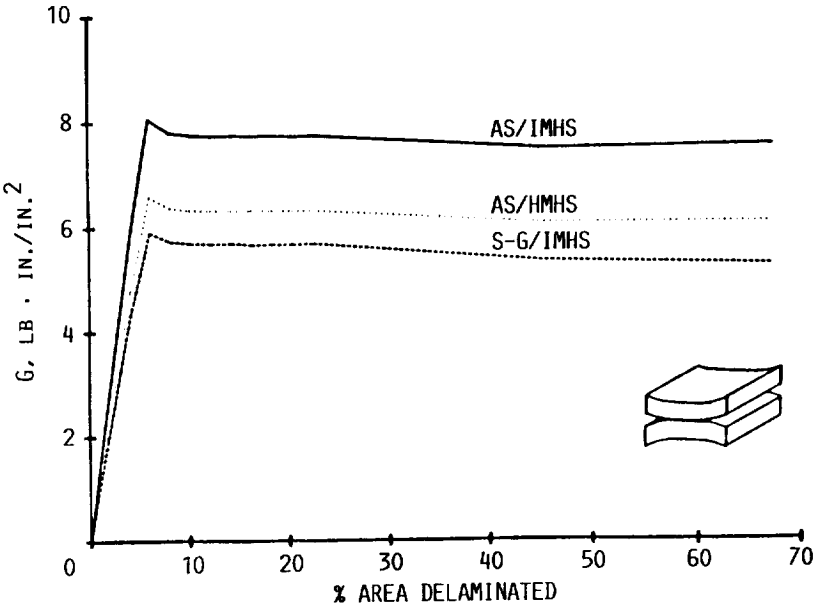

FIGURE 11. - STRAIN ENERGY RELEASE RATE 14-PLY CENTER DELAMINATION.

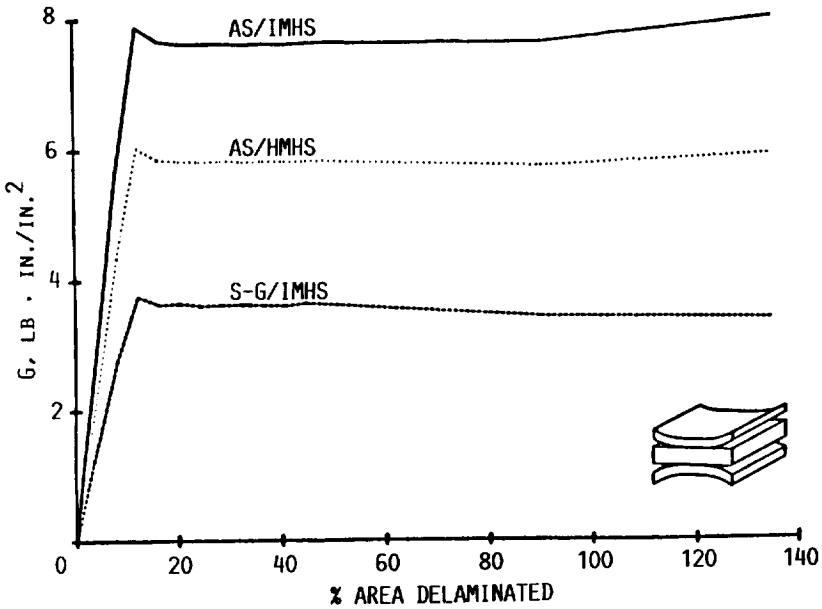

FIGURE 12. - STRAIN ENERGY RELEASE RATE 14-PLY OFFSET DELAMINATION.

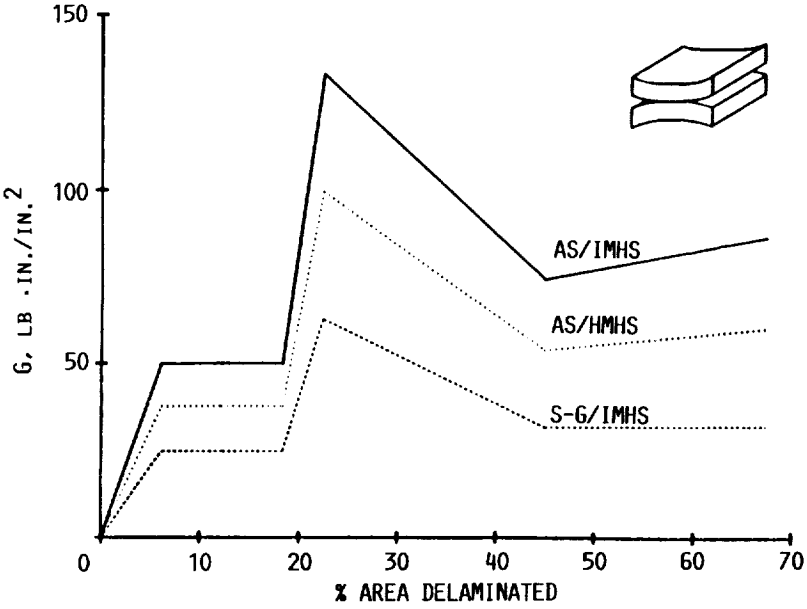

FIGURE 13. - STRAIN ENERGY RELEASE RATE 6-PLY CENTER/ POCKET DELAMINATION.

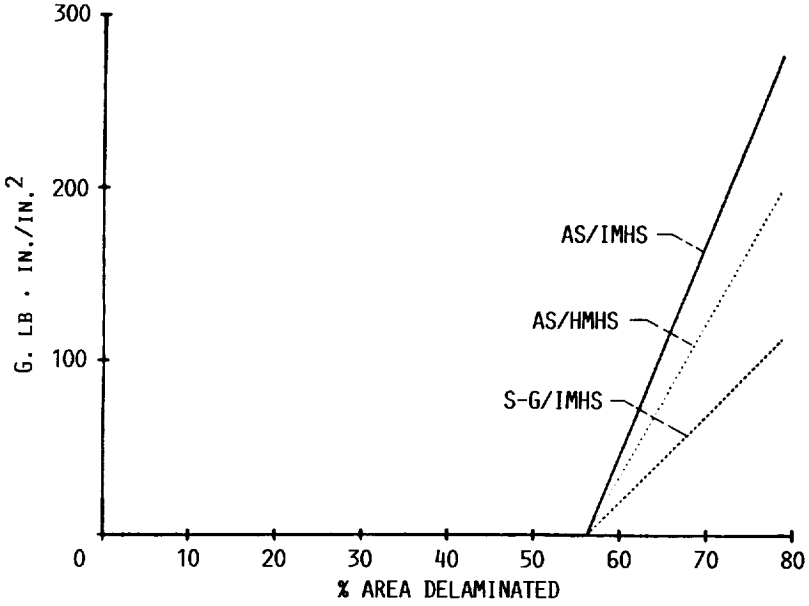

FIGURE 14. - STRAIN ENERGY RELEASE RATE 6-PLY INTERIOR/ CENTER DELAMINATION.

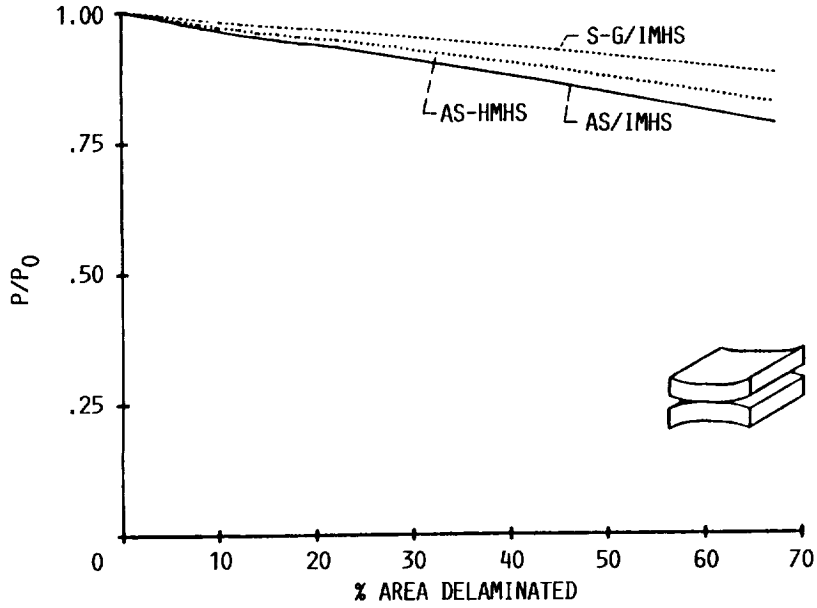

FIGURE 15. - BUCKLING LOAD 6-PLY CENTER DELAMINATION (SIMILAR BEHAVIOR FOR AXIAL STIFFNESS AND VIBRATION FREQUENCY AND COMPLEMENTARY BEHAVIOR FOR END DISPLACEMENT).

NASA
National Aeronautics and Space Administration

Report Documentation Page

1. Report No.	2. Government Accession No.	3. Recipient's Catalog No.
NASA TM-101415		

4. Title and Subtitle

Fracture Toughness Computational Simulation of General Delaminations in Fiber Composites

5. Report Date

6. Performing Organization Code

7. Author(s)

T.E. Wilt, P.L.N. Murthy, and C.C. Chamis

8. Performing Organization Report No.

E-4513

10. Work Unit No.

505-63-11

9. Performing Organization Name and Address

National Aeronautics and Space Administration
Lewis Research Center
Cleveland, Ohio 44135-3191

11. Contract or Grant No.

13. Type of Report and Period Covered

Technical Memorandum

12. Sponsoring Agency Name and Address

National Aeronautics and Space Administration
Washington, D.C. 20546-0001

14. Sponsoring Agency Code

15. Supplementary Notes

Presented at the 29th Structural Dynamics and Materials Conference cosponsored by the AIAA, ASME, AHS, and ASC, Williamsburg, Virginia, April 18-20, 1988. T.E. Wilt, Akron University, Akron, Ohio 44325; P.L.N. Murthy, Cleveland State University, Cleveland, Ohio 44115 and NASA Resident Research Associate; C.C. Chamis, NASA Lewis Research Center.

16. Abstract

A procedure is described to computationally simulate composite laminate fracture toughness in terms of strain energy release rate (SERR). It is also used to evaluate the degradation in laminate structural integrity in terms of displacements, loss in stiffness, loss in vibration frequencies and loss in buckling resistance. Specific laminates are selected for detailed studies in order to demonstrate the generality of the procedure. These laminates had center (midplane) delaminations, off-center delaminations, and pocket delaminations (center and off-center) at the free-edge and center delaminations at the interior. The laminates had two different thicknesses and were made from three different materials. The results obtained illustrate the effects of delamination on the laminate structural integrity and on the laminate strain energy release rate (composite fracture toughness).

17. Key Words (Suggested by Author(s))	18. Distribution Statement
Finite element; Multi-point constraints; Stress analysis; Structural integrity; Axial displacements; Buckling; Vibration frequency; Laminate stiffnesses; Uniform delaminations; Pocket delaminations; Multiple delalminations; Interior delaminations; Degradation rate; Fracture mechanics; Strain energy release rate; Composite materials	Unclassified – Unlimited Subject Category 24

19. Security Classif. (of this report)	20. Security Classif. (of this page)	21. No of pages	22. Price*
Unclassified	Unclassified	18	A03

NASA FORM 1626 OCT 86

*For sale by the National Technical Information Service, Springfield, Virginia 22161

National Aeronautics and
Space Administration

Lewis Research Center
Cleveland, Ohio 44135

SECOND CLASS MAIL

ADDRESS CORRECTION REQUESTED

Official Business
Penalty for Private Use $300

Postage and Fees Paid
National Aeronautics and
Space Administration
NASA-451

NASA